ON THE TEMPORAL VARIABILITY OF THE SEA SURFACE TEMPERATURE IN THE SOUTHWESTERN ATLANTIC BASED ON THE ANALYSIS OF "PATHFINDER AVHRR/NOAA" IMAGES

Variabilidade temporal da temperatura da superfície do mar do Atlântico Sudoeste baseado na análise de imagens Pathfinder AVHRR/NOAA

Carlos E. P. Teixeira [1,2,*]
Mauricio M. Mata[2]
Carlos A. D. Lentini[3]
Carlos A. E. Garcia[2]
Edmo J. D. Campos[1]

[1] Universidade de São Paulo - USP
Laboratório de Modelagem Numérica, Instituto Oceanográfico
Praça do Oceanografico, Cidade Universitaria, São Paulo, SP, 05508-900, Brasil
teixeira.carlos@saugov.sa.gov.au
edmo@io.usp.br

[2] Fundação Universidade Federal de Rio Grande - FUFRG
Laboratório de Oceanografia Física, Departamento de Física
Av. Italia, Km 8, Campus Carreiros, Rio Grande, RS, 96201-900, CP 474, Brasil,
mauricio.mata@furg.br
dfsgar@furg.br

[3] Universidade Federal da Bahia - UFBA
Depto. Fisica da Terra e do Meio Ambiente - Instituto de Física
Travessa Barão de Jeremoabo, s/n, Campus Ondina, Salvador, BA, Brasil 40170-280, Brasil,
clentini@ufba.br

*** Present Address:**
South Australia Research and Development Institute
Aquatic Sciences
2nd Hamra Av., West Beach, Adelaide, SA, Australia

ABSTRACT

This study uses nine years of daily 9-km Pathfinder AVHRR/NOAA Sea Surface Temperature (SST) images to estimate the SST temporal variability of the southwestern Atlantic Ocean on time-scales ranging from sub-seasonal to inter-annual. First, we evaluated the annual and semi-annual deterministic signals in the total variability of the SST fields using a least-squares fit. We then removed the annual and semi-annual components from the original data and used a low-pass filter to estimate the contribution of the inter-annual component of total variability. Finally, the inter-annual signal was removed and the variance associated to the remaining residuals was calculated to address the intra-annual component. The annual signal was found to dominate over the area with a coefficient of determination higher than 85%, with amplitudes ranging from 1° to 13°C. The largest amplitudes were found on the continental shelf, with the highest values near the La Plata River estuary as a consequence of the river runoff. The semi-annual signal was significant near the Brazil/Malvinas Confluence (BMC), due to mesoscale activity with same periods. The Southern Annular Mode (SAM) appeared to be related to the high values of semi-annual amplitudes found close to 50º S, 65º W. The results for the oceanic area north of BMC showed that the region between 24°S and 32°S had semi-annual amplitudes close to 1.5°C. We suggested that this high amplitude was related to the South Atlantic Convergence Zone. The domain, as a whole, experienced weak inter-annual variations, except in the vicinity of the BMC where higher

values (~1.2º C) were found. The Argentine shelf and the South Brazil Bight also presented significant inter-annual variability related to the inter-annual variations in the La Plata river discharge forced by ENSO events. The region close to the BMC and the South Atlantic Current were associated with high intra-annual variances due to intense mesoscale activity normally observed in these areas. Low intra-annual variance found in the Zapiola Drift was related to the anticyclone flow in this region which tended to isolate the circulation in the center of the drift. This gyre was forced by the meso-scale events of the BMC and the Antarctic Circumpolar Current that appeared as high values of intra-annual variance around the Zapiola Drift. The higher resolution SST data set, the longer time series and the larger domain permitted to identify new and important oceanographic features and to extend the results already reported in the southwestern Atlantic.

Keywords: Southwestern Atlantic, SST, Brazil Current, Brazil-Malvinas Confluence, AVHRR-Pathfinder, Zapiola Drift.

RESUMO

No presente estudo, nove anos de imagens diárias da temperatura da superfície do mar (TSM) do tipo Pathfinder AVHRR/NOAA, com resolução espacial de 9x9 quilômetros, são utilizadas para estimar a variabilidade temporal da TSM para o setor Sudoeste do Oceano Atlântico. São analisadas escalas temporais variando de intra-sazonal a inter-anual. Inicialmente, foi estimado o sinal determinístico (ciclo anual + semi-anual) da variabilidade total dos dados através da metodologia de mínimos quadrados. Este sinal foi então subtraído dos dados originais e um filtro passa baixa foi aplicado para avaliar a contribuição do componente inter-anual da variabilidade total. Finalmente, o sinal inter-anual também foi removido e a variância do sinal residual calculada a fim de se estimar a componente intra-anual da variabilidade. Os resultados demonstram que o sinal anual explica a maior parte da variabilidade da TSM na região de estudo, com um coeficiente da determinação maior do que 85% e com amplitudes que variam de 1° a 13°C. As maiores amplitudes do ciclo anual são encontradas na plataforma continental, com os valores máximos ocorrendo junto a estuário do Rio da Prata como uma consequência dos desagúes continentais. O sinal semi-anual é significante na região da Confluência Brasil – Malvinas (CBM) devido à atividade de meso-escala com este mesmo período de variabilidade presente na região. O *Southern Annular Mode* (SAM) parece estar relacionado com os altos valores de amplitude semi-anual encontrados na região próxima 50º S, 65º W. Novos resultados para região oceânica ao norte da CBM demonstram que a região entre 24°S e 32°S apresenta amplitude do ciclo semi-anual próxima a 1,5 ºC. Sugere-se que estes altos valores de amplitude estão relacionados com a Convergência do Atlântico Sul. Em geral a região de estudo apresenta uma variabilidade inter-anual pequena, com exceção da CBM onde os valores máximos (~ 1,2°C) são encontrados. A plataforma continental Argentina e a Baia de Santos também apresentam variabilidade inter-anualsignificativa relacionada com as mudanças no deságue do Rio da Prata forçadas pelos eventos ENOS. As regiões próximas à CBM e da Corrente do Atlântico Sul estão associadas com valores de variância intra-anuais relativamente elevados, devido à intensa atividade do mesoscale observada nestas áreas. A baixa variância intra-anual encontrada no Zapiola *Drift*, esta relacionada a fluxo anticiclônico presente nesta região que tende a isolar a circulação no centro do *"Drift"*. Este giro é forcado pelos eventos de meso-escala da CBM e da Corrente Circumpolar Antártica os quais aparecem como alto valores de variância intra-anual ao redor do Zapiola Drift. A maior resolução do banco de dados de TSM, a maior série temporal e o maior domínio permitiram estender os resultados já apresentados para a região do Atlântico Sudoeste e identificar novas e importantes feições oceanográficas.

Palavras chaves: Atlântico Sudoeste, TSM, Corrente do Brasil, Confluência Brasil – Malvinas, AVHRR-Pathfinder, Zapiola Drift.

1. INTRODUCTION

The sea surface temperature (SST) is a very important oceanic variable because it determines the exchange of heat with the overlying atmosphere, acts as an indicator of the distribution of a large variety of marine species and serves as an important tracer of several oceanographic processes, which have a surface thermal signature. Among these processes are the coastal upwelling, mesoscale phenomena (eddies, rings and meanders) and oceanic fronts. Furthermore, SST plays an important role in the study of ocean-atmosphere interactions and in the determination of the variability of the climatic conditions, both in regional and global scales (CRACKNELL and HAYES, 1990).

Several studies have investigated the importance of SST variability in the South Atlantic with respect to climate (VENEGAS *et al.*, 1997; ACEITUANO *et al.*, 1988; DIAZ *et al.*, 1998; PAEGLE and MO, 2002). However, due to the lack of in situ data, such variability is not well understood as it is in the North Atlantic. Given the importance of the South Atlantic in the meridional heat transfer to the northern hemisphere and to the regional climate, a better understanding of the SST variability in that area is essential. Variability of SST fields occurs over all spatial and temporal scales and is controlled mainly by

the seasonal distribution of solar radiation. The wind regime over the ocean, river discharge and strong oceanic western boundary currents also impose significant variability on the SST field.

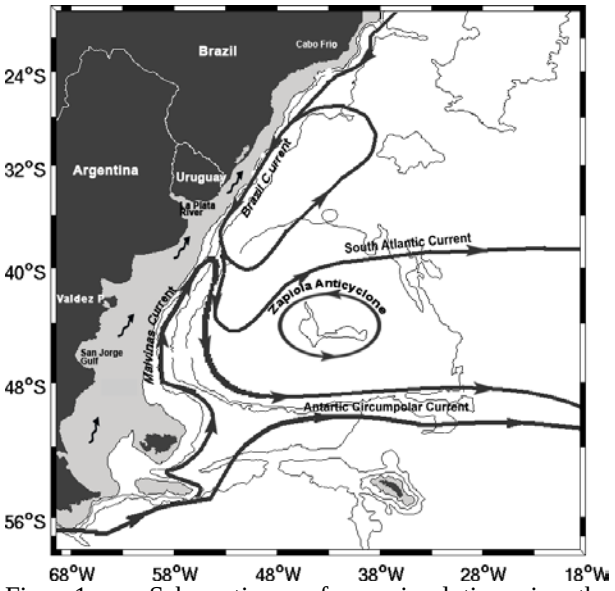

Fig. 1 - Schematic surface circulation in the Southwestern Atlantic shelf (adapted from STRAMMA and ENGLAND, 1999; ROMERO *et al.* 2006). Contours correspond to the 200 (shaded), 1000, 3000 and 5000 m isobaths.

The dynamics in the offshore region of the Southwestern Atlantic (SWA) is dominated by the poleward flow of the Brazil Current (BC), which carries warm and saline tropical waters, and the Malvinas Current (MC), a highly barotropic current which transports cooler and fresher Sub-Antarctic Water (SAW) towards lower latitudes (Fig. 1). The region between 38°-40°S where these two western boundary currents meet is known as the Brazil-Malvinas Confluence (BMC) and is one of the most energetic regions of the world ocean (e.g.: LEGECKIS and GORDON, 1982; GORDON, 1989; CHELTON *et al.*, 1990). Conversely, the continental shelf and coastal waters off Uruguay and Southern Brazil are strongly influenced by the freshwater plumes of the La Plata River and the Patos-Mirim Lagoon system (PIOLA *et al.*, 2000; LENTINI *et al.*, 2001; PIOLA *et al.*, 2005;). Off the Argentinean coastline, the inner shelf is dominated by waters from the confluence region and from the Magellan Strait outflow further south (GLORIOSO, 1987).

In studies of basin-scale phenomena, for which in-situ data coverage is insufficient and/or very expensive, an alternative way of measuring SST is by remote sensing platforms. Nowadays, these measurements allow an adequate quasi-synoptic evaluation of the SST field with the necessary precision and accuracy. Among a variety of sensors and platforms capable of measuring the SST field in the ocean, one that is mostly used is the Advanced Very High Resolution Radiometer (AVHRR), which flies on board of the NOAA-n polar orbit satellites. This sensor measures the radiance reflected/emitted by the surface of the planet in wavelength bands from the visible to the infrared spectra. However, satellite SST measurements are affected by the presence of clouds and aerosols in the atmosphere, which can generate errors or make SST-retrievals impossible. In order to minimize this problem, the Jet Propulsion Laboratory (JPL) developed the "Pathfinder best SST" algorithm which presents a precision of 0.1º C and a RMS of 0.94º C (e.g. SMITH *et al.*, 1996; KILPATRICK *et al.*, 2001).

In this study, the SST variability in SWA for the region delimited by 18ºS – 58ºS and 18ºW – 70ºW is investigated using 3285 daily SST images from the "Pathfinder best SST", version 4.1, with a spatial resolution of 9km x 9 km, covering the period from January 1993 to December 2001. The annual and semi-annual harmonics, which correspond to the deterministic part of the SST signal, are fitted to the original data using a least-square scheme. The SST residuals from this fit are the basis of all subsequent analyses. The present work is presented as follows.. Data and methods are described in the section 2. The results are presented in Section 3 and are the basis of the subsequent discussion. Finally, summary and conclusions are presented in Section 4.

2. DATA AND METHODS

In this work we used daily "Pathfinder best SST" data, version 4.1 images (SMITH *et al.*, 1996; KILPATRICK *et al.*, 2001), with a spatial resolution of 9 km, obtained from JPL Physical Oceanography Distributed Active Archive Center (PO.DAAC, http://podaac.jpl.nasa.gov). These digital data are derived from Global Area Coverage (GAC) images, collected by the AVHRR sensor flying onboard the NOAA-n satellites. In the "Pathfinder best SST" dataset, clouds and aerosol effects are minimized by the pathfinder algorithm (SMITH *et al.*, 1996; KILPATRICK *et al.*, 2001). Flags are attributed to each pixel, which vary from 0 (maximum contamination) to 7 (minimum contamination). Only pixels flagged with values of 3 or higher are considered. The remaining pixels receive a mask and are characterized as gaps. Furthermore, the algorithm performs a temporal and spatial comparison with the adjacent pixels. If the difference between the central and adjacent pixel is over 2ºC, the first is characterized as cloud. The pathfinder algorithm presents clear advantages in the SST temporal analysis when compared to other methods and despite the fact it produces large amount of gaps, the post-processed images are very accurate and carry very little cloud contamination. A detailed description of the algorithm can be found in KILPATRICK *et al.* (2001).
The 9-yr time series of SST fields are extracted for each pixel of the image (456 X 638 pixels) and are analyzed separately. As the time series corresponding to each pixel has 3285 observations, the resulting data volume is 3285 x 456 x 638 records. Basic statistics and

percentage of valid data (ratio between number of gaps and observed data) are also estimated for the entire period for each series prior to the least-squares fit.

The analysis of the annual and semi-annual harmonics is then carried out in order to characterize the deterministic portion of the SST variability. For this, a least-squares method is used (Emery and Thomson, 1998) and defined as:

$$x(t_n) = \bar{x} + C_q \cos\left[(2\pi/T)(t_n - \varnothing_q)\right] + x_r(t_n)$$

Here $x(t_n)$ is the temperature at a given instant t_n, $\bar{x}$ is the mean SST value, C_q the amplitude of harmonic with period T, $\varnothing_q$ is the phase and $x_r(t_n)$ is the residual from the fit, comprised of non-detected periodic signals and by the sampling noise. The time t_n varies from t_1 (first sampling day) to t_{3285} (last sampling day). The above equation is justified for the analysis as the annual variability of solar radiation possesses a sinusoidal behavior and is the main forcing of the SST in tropical and subtropical regions (SECKEL and BEAUDRY, 1973; PODESTÁ *et al.*, 1991; PROVOST *et al.*, 1992; LENTINI *et al.*, 2000). Similar methodology has been used successfully with ocean color data in the same area (GARCIA *et al.*, 2004).

Based on previous studies in the region, two models are initially fitted to the original dataset to capture the deterministic portion of the SST temporal variability: (i) model A, which corresponds to the fit of the annual harmonic (T_{annual} = 365.25 days) and (ii) model AS, where the annual and the semiannual harmonics are included (T_{annual} = 365.25 + $T_{semi\text{-}annual}$ = 182.62 days). An estimate of the goodness of fit for each harmonic was obtained by examining the determination coefficient (R^2) between the original and modeled data.

Next, we estimate the inter-annual contribution to the total SST variability in the region by initially removing the annual and semi-annual contribution from the original SST fields. The residuals from the fit, considered here mostly a contribution to the SST inter-annual variability, is subject to an objective analysis with a decorrelation time scale of 365 days in order to filter out frequencies higher than one year. The low-pass filter with cutoff frequency corresponding to one year (CHELTON and SCHLAX, 1991; WALKER and WILKIN, 1998) is used in the objective analysis because, unlike the running mean filter, it preserves most of the low frequency energy of a particular time series giving better results. The standard deviation of the filtered series is then used as an estimate of the amplitude of the inter-annual variability of the SST in the study area. Although the method does not allow any inferences regarding the time scale contribution to the inter-annual variability, it provides an overview of the spatial distribution and relative importance of this component to the total SST signal (WALKER and WILKIN, 1998).

Finally, the inter-annual contribution (i.e. the filtered time series) is also removed from the SST residuals. Therefore, the remaining variability should contain basically the intra-annual variability and the sampling noise. The variance of these residuals were used as an estimate of the SST variability due to the intra-annual phenomena.

According to different hydrodynamic regimes found in the area of study, 12 points are selected for a detailed analysis of the regression fit of these SST time series, which shall be used throughout this work. The position of each point is listed in Table 1 and is indicated in the maps.

3. RESULTS AND DISCUSSION

3.1 - Valid data, mean and standard deviation:

The percentage of valid data for each pixel throughout the 3285 days analyzed is presented in figure 2. The same results are presented for the 12 sites in the table 1. Most of the study area has low percentages of valid data, which can be attributed to the conservative character of the Pathfinder algorithm. The mean value of valid data for the role period is 16%, but it can reach higher values (ex.: sites 1 and 10) in coastal regions as well as the locations under the sole influence of the MC (site 11). Lowest values are found in the BMC region (sites 6 and 8), the Subantartic Front (site 12) and in the southeast area of the domain. In this region, the low percentage of available data is mainly due to the intense cloud coverage in the southeast region (GAN, 1991), although the presence of mesoscale events associated or not with thermal fronts with gradients over 2ºC/9km, may be erroneously characterized as clouds by the SST pathfinder algorithm (VIVIER and PROVOST, 1999; SARACENO *et al.* 2004; SARACENO and PROVOST, 2005)..

The number of valid data is highest in the austral summer, with a mean value of 24% and lowest in the winter (14%). The same seasonal difference (~ 10%) was found by SARACENO *et al.*, 2004. The inter-annual difference in the percentage of available data is lower than 2% for the 9 years of observations.

The influence of the number and the temporal distribution of the gaps on the results are tested in two ways. In the first test, a synthetic time series is created using Equation 1 with prescribed amplitudes and phases, representing the annual and semi-annual cycle, plus a low-passed series, representing the inter-annual contribution, plus a white signal, representing the intra-annual variability. Next, this continuous time series is filled with 95% of gaps uniformly distributed in time. Finally, the annual and semi-annual amplitudes and their associated phases, the R^2 coefficient, the inter-annual variability and the intra-annual variance are evaluated for the continuous and the gapped time series. The comparison between these two tests shows that with percentage of 95% of gaps there were no differences in the amplitudes, phases and R^2 results, and a small

difference (lower than 4%) in the inter-annual variability and intra-annual variance.

In the second test, the potential impact of the seasonal difference in the distribution of the gaps is examined. The above test is repeated, except that now the amplitudes, phases and the inter-annual component of each of the 12 sites plus a white noise are used to create 12 continuous series. The same amount and distribution of gaps for site 12, which contains the large number of gaps, are fitted in each series. Results show that there were no differences in the amplitude and phase results, except an increase of 8% in the differences for the inter-annual variability and intra-annual variance. A small difference in the R^2 coefficient (lower than 3%) is also observed.

The tests described above show that the low number of valid data and the seasonal differences in the distribution of the gaps do not affect our results.

Table 1 - Geographical positions (see Fig. 3) and percentage of valid data (%).

Site	Lat (S)	Lon (W)	Pc
1	23º40’	44º 30’	26.67
2	25º30’	45º	22.86
3	25º30’	48º10’	22.61
4	29º10’	49º20’	22.12
5	35º	54º30’	27.25
6	39º	54º30’	12.36
7	42º	58º	29.81
8	43º	54º30’	15.14
9	45º	45º	16.30
10	46º	67º	33.00
11	48º10’	60º30’	30.12
12	48º30’	44º30’	9.31

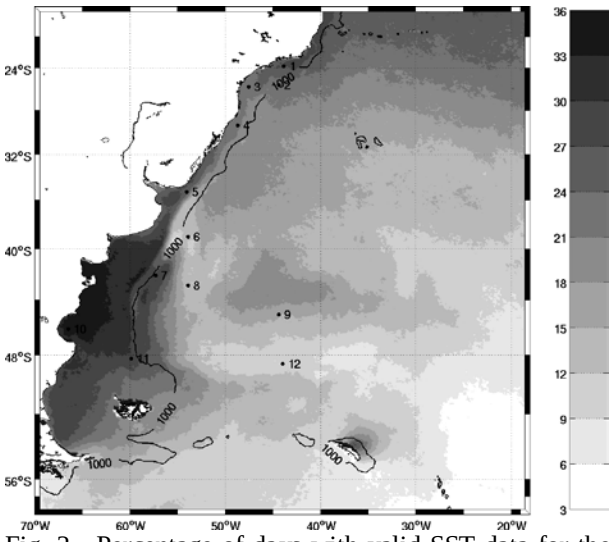

Fig. 2 - Percentage of days with valid SST data for the period 1993 - 2001.

Based on mean SST for the period of study, the thermal signature of the BC is marked by high temperatures close to the continental slope (SST > 23 ºC), whereas the MC, with temperatures lower than 7ºC, can be observed along the Argentine continental slope (Fig. 3). In the south of Brazil and Uruguay, the continental shelf is distinguished by the presence of a thermal signature with SST varying between 17 and 19°C, associated to the discharge of the La Plata River and the Patos Lagoon (e.g. SOARES and MOLLER, 2001). This thermal feature, which appears well marked in the mean SST image (Fig. 3), also has a very noticeable seasonal cycle following river runoff and wind stress variability. Maximum northward penetration occurs during austral winter/spring (PIOLA *et al.*, 2005). The semi-stationary meander of the BC retroflection (e.g. CAMPOS and OLSON, 1991; LENTINI *et al.*, 2006) appears as a “U” shaped pattern (near 42ºS, 52º W) with temperatures around 18ºC. The meander marks the western edge of the Subtropical Front in the South Atlantic Ocean (TOMCZAK and GODFREY, 1994). The Antarctic Circumpolar Current (ACC) SST signature, with water temperatures below 1ºC, can also be observed in the extreme south of the SWA domain (Fig. 3).

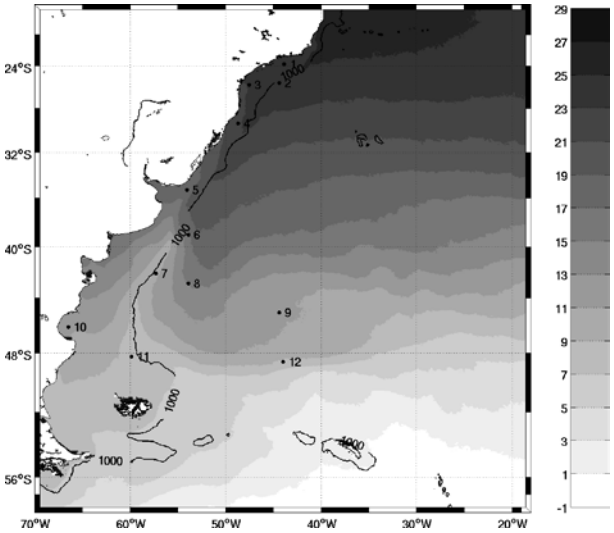

Fig. 3 - Mean SST values for the period 1993 - 2001. Units in ºC.

The standard deviation of the mean SST field is shown in figure 4. The highest values occur in the region of the La Plata River discharge, indicative of the influence of the thermal variability of its waters over the adjacent shelf. Overall, the highest deviations from the mean occur over the continental shelf due to the fact that it is relatively shallow and thus responds faster to seasonal variations in solar energy, and to wind and tidal mixing when compared to open ocean areas. Farther offshore, the mesoscale eddies shed in the BMC confer a high variability to the SST signal (GARZOLI and BIANCHI, 1987; GARZOLI and GIULIVI, 1994; LENTINI *et al.*, 2002; 2006; DE SOUZA *et al.*, 2006).

Minimum values of standard deviation are observed over the Argentine shelf, especially near the San Jorge Gulf (site 10, 46ºS, 66º 30 ’W) and the

Valdez Peninsula (41º 30 'S, 65 ºW). Both regions have strong tidal currents (GLORIOSO and FLATHER, 1997) which tend to homogenize the water column and diminish the SST variability throughout the year (GLORIOSO, 1987; ROMERO *et al*. 2006).

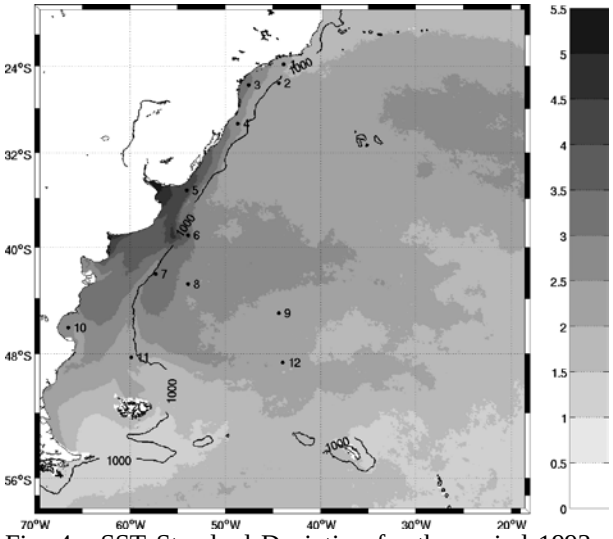

Fig. 4 - SST Standard Deviation for the period 1993 - 2001. Units in ºC.

3.2 - Characterization of the annual and semi-annual cycles:

Table 2 presents the annual plus semi-annual model parameters, amplitude, phase and determination coefficient (R^2), and also the inter-annual variability and intra-annual variance that will be discussed in the following sections.

Table 2 - Parameters obtained for each site by using the deterministic model constituted of annual plus semi-annual periods (model AS). AA = amplitude of the annual cycle (ºC). AAS = amplitude of the semiannual cycle (ºC). PhA = phase of the annual cycle (days). R^2 = determination coefficient between the original data and the model. (%). Inter = Inter-annual variability (ºC). Intra = Intra-annual variance (ºC²).

Site	AA	ASA	PhA	R^2	Inter	Intra
1	5.6	0.7	50	88	0.4	1.0
2	5.1	0.4	51	91	0.3	0.5
3	8.7	0.4	36	90	0.3	1.2
4	7.9	0.6	36	90	0.3	1.0
5	11.7	0.4	35	93	0.3	1.0
6	9.6	0.3	35	79	1.0	2.4
7	7.4	0.6	36	92	0.4	0.7
8	6.4	1.0	38	79	0.4	2.6
9	5.7	0.6	54	92	0.4	0.5
10	7.7	0.4	36	92	0.4	0.4
11	5.9	0.9	34	90	0.3	0.4
12	5.1	0.2	53	74	0.8	1.6

The performance of the two proposed seasonal models is evaluated separately. As it can be observed in the R^2 map between the original data and the annual plus semi-annual cycle model (model AS), there is a realistic fit to the original data (Fig. 5). When the semiannual harmonic (model A) is not included, the R^2 coefficient is slightly small (not shown). The highest differences are of the order of 3 %, and are related to the oceanic region between 24 and 40º S, and the southern portion of the SWA domain, where the semiannual cycle relative importance to the total signal increases.

From the southern limit of the domain up to 24 ºS, the continental shelf presents the highest values of R^2. Further to the north, the shelf is possibly affected by mesoscale events of the BC caused by the sudden interruption in the orientation of the isobaths of the continental slope near Cabo Frio (22 ºS) (LENTINI, *et al*., 2000). Moreover, the region off Cabo Frio is marked by a seasonal upwelling, which confers a non-deterministic characteristic to the SST signal in that area, thus lowering the values of R^2 (Fig. 5). Low values of R^2 also appear in the region of the BMC (sites 6 and 8) and subantartic front (site 12) due to the mesoscale activity (GARZOLI and BIANCHI, 1987; GARZOLI and GIULIVI, 1994; VIVIER and PROVOST, 1999; GARCIA *et al*. 2004; LENTINI *et al*., 2001; 2002; 2006).

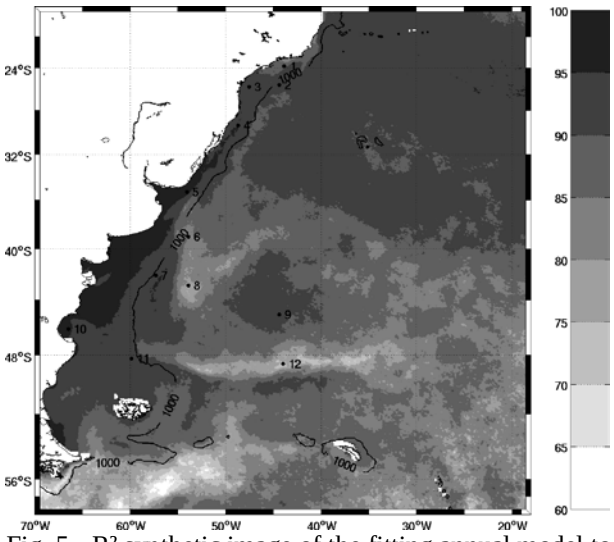

Fig. 5 - R^2 synthetic image of the fitting annual model to observed SST fields (relative units)

The SST time series and the seasonal fits, annual plus semiannual harmonics, are presented in figure 8. Overall, there is a good adjustment for all the sites. Based on this figure, one can observe (i) the efficiency of the model is not associated with the number of valid SST data, as (ii) the data is evenly distributed throughout almost all the time series and (iii) the presence of mesoscale events in the region, which confers a non-deterministic characteristic to the SST cycle. The best fit occurs at sites 5, 9 and 10 with R^2 > 92%. Those points are associated with low mesoscale activity, such as the continental shelf in front of the La

Plata River (site 5), the San Jorge Gulf (site 10) and the Zapiola Drift (site 9). The worst fit occurs at sites 6, 8 and 12 where less than 80% of the total variance of the original SST data can be explained by the model fit. Those sites present a high mesoscale dynamics with negative consequences to the model performance, clearly seen in the time-series plots by the scattering of the residuals around the adjusted annual cycle (Fig. 8) and the low-passed component (Fig. 12).

The synthetic images of the amplitude and phase of the annual cycle can be seen in figures 6 and 7, respectively. A large variation of SST fields exists over the Argentine continental shelf and north of the La Plata River mouth (site 5), reaching over 10 ºC (Fig. 6). These large values are probably a consequence of the northward advection of waters from the Patagonian shelf (south of 40 ºS) (ROMERO *et al.*, 2006) and the La Plata River runoff, respectively. Low values of SST amplitude occur in the San Jorge Gulf (site 10) and the Valdez Peninsula and, as discussed above, they are the result of the interaction of the tidal currents with the ocean bottom that tends to mix the water column and thus decreases the SST variability throughout the year.

Along the continental slope south of 40 ºS, the influence of the MC is marked, with lower amplitudes than the adjacent waters within less then 8ºC. Conversely, the ocean region between 34ºS and 40ºS has a large annual harmonic as a result of the seasonal meridional migration of the BMC (OLSON *et al.*, 1991; LENTINI *et al.*, 2002), which has also been observed in the analysis of variations of chlorophyll-a concentration in the region (GARCIA *et al.*, 2004).

Similar amplitude values were found by PODESTA *et al.*, 1991, when analyzing four years of five-day composite SST data to the region between 34º and 50º S, and 50ºW and the South America coast.

A synthetic image of the phase of the annual cycles is presented in figure 7. The phase is referenced to the 1st of January. The continental shelf break separates regions with distinct phases. The highest values of SST occur earlier (between 35 and 45 days) over the shelf, since they are shallower and therefore respond faster than open ocean areas to variations in solar irradiance. Additionally, the region is subject to the influence of relatively warm waters discharge from both the La Plata River and the Patos Lagoon estuaries, and from a strong mixing regime during the austral winter. Over the continental shelf and north of 24 ºS, the phase of maximum temperature occurs later between 50 and 60 days, which is expected as the seasonal cycle of heating/cooling imposes large and well defined variability to mid- latitudes when compared to lower-latitudes. Furthermore, such phase delay may also be associated to the mesoscale events forced by the meandering of the BC, which frequently occurs in this region (CAMPOS *et al.*, 1995), and with the northeast wind-induced upwelling via coastal Ekman transport, common during the austral summer months.

A "U" shaped pattern, with maximum temperature occurring between 35 and 45 days, is observed close to the BMC region. This pattern is in phase with the continental shelf, due to the advection of coastal waters to the oceanic region (recently reported by GONZALEZ-SILVERA *et al.* 2006 and ROMERO *et al.* 2006).

In the southern part of the domain, the maximum temperature occurs with a delay of 25 to 30 days due to the advection of subantarctic surface waters, which are relatively warmer during austral summer. Melting waters from the Magellan Strait also influence the coastal area near 55º S (GLORIOSO, 1987; RIVAS, 1994) locally delaying the summer solar heating.

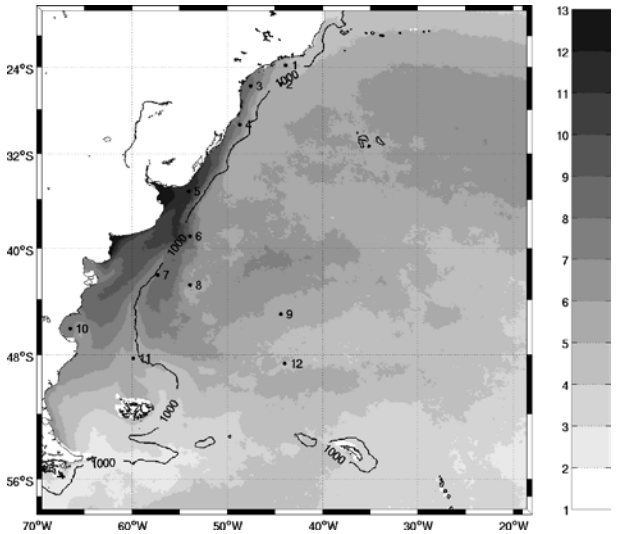

Fig. 6 - Amplitude of the modeled annual cycle. Units in ºC.

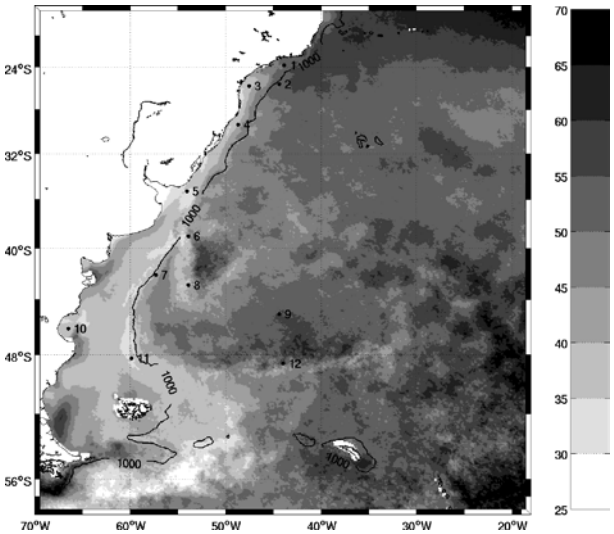

Fig. 7 - Phase of the modeled annual cycle (units are days from 1 January).

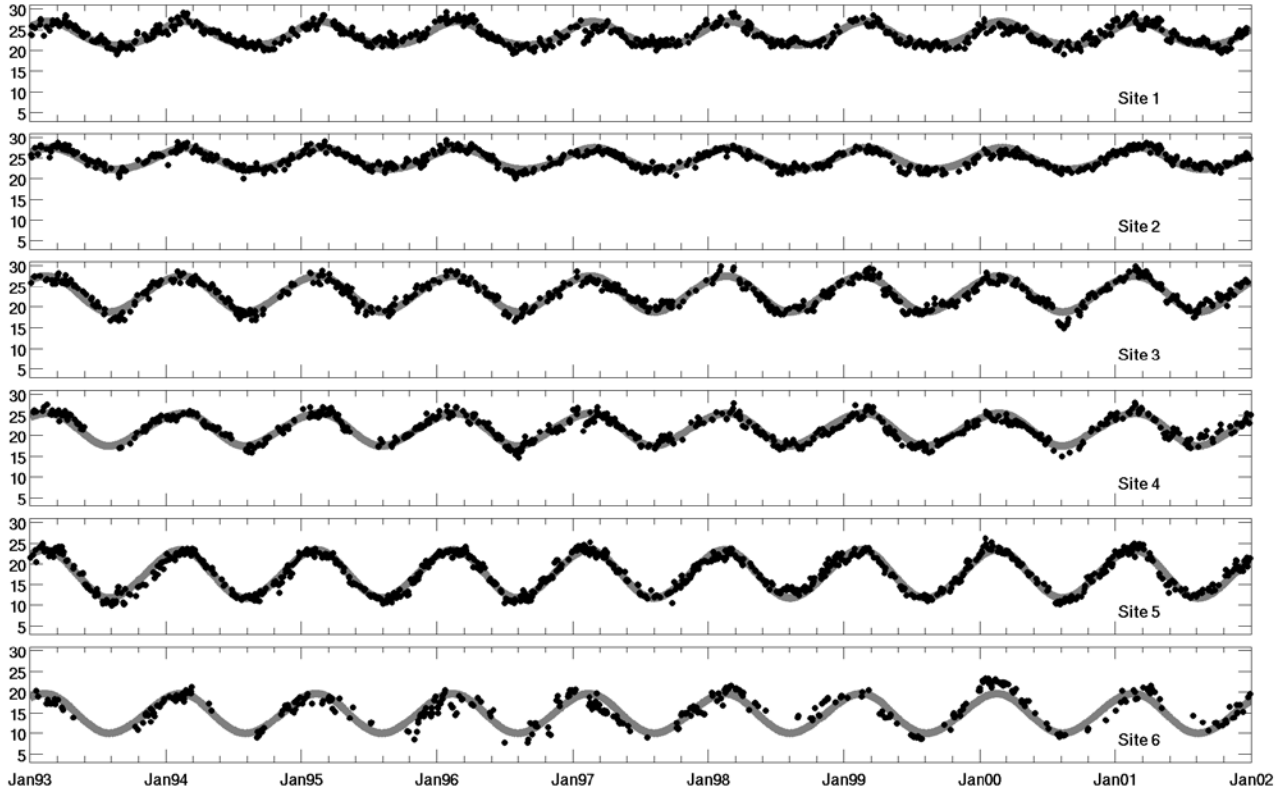

Fig. 8a - 'Pathfinder' SST observations (points) and estimated annual SST cycle (line). Sites from 1 to 6. Units in ºC

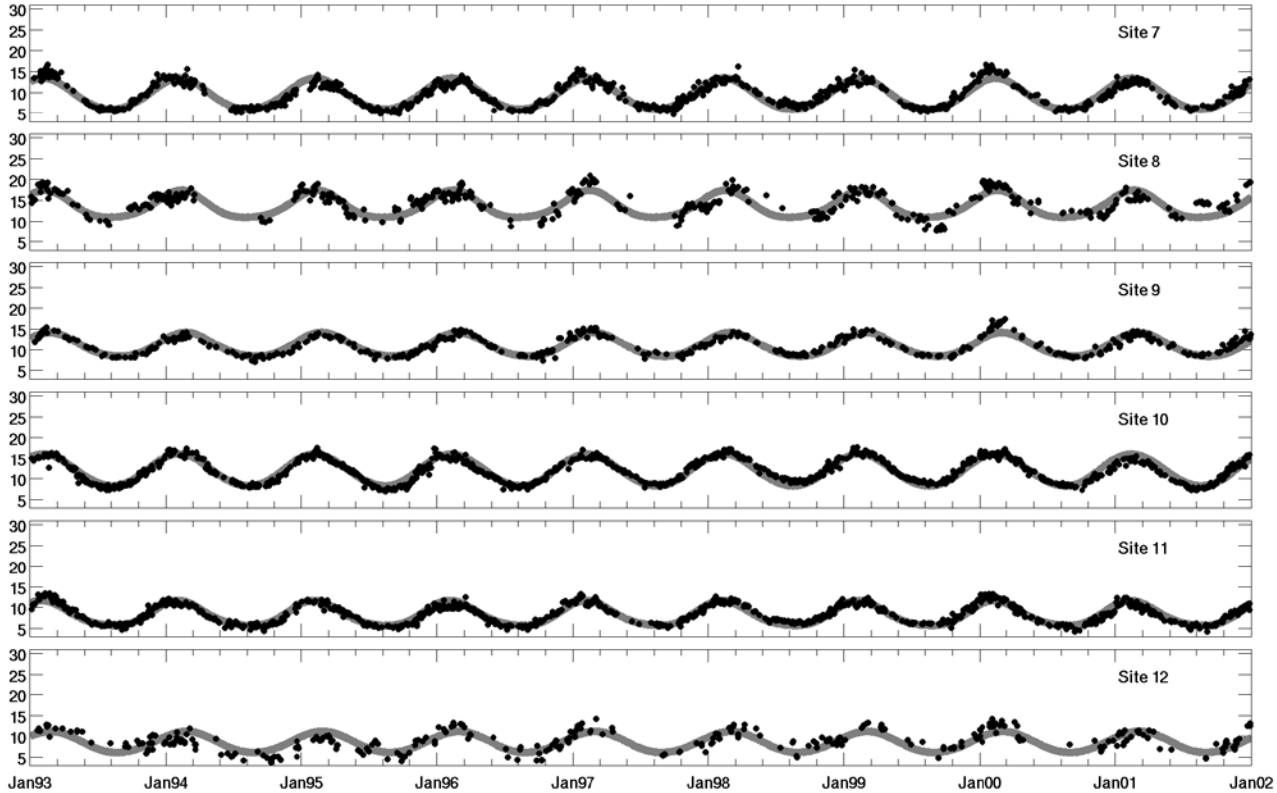

Fig. 8b - 'Pathfinder' SST (points) and estimated annual SST cycle (line). Sites from 7 to 12. Units in ºC

The synthetic image of the semi-annual amplitudes is shown in figure 9. The southwestern part (50º S, 65ºW) of the Southwestern Atlantic domain have significant values of semi-annual amplitudes. Similar values of amplitudes were found by PROVOST *et al.*, 1992 in the BMC and in the southwestern part of the SWA domain examining 3 years of 5-day composite SST. These authors associated the relative high

amplitudes to the frontal motions of the BMC and to a half-year wave observed by VAN LOON (1966) in various fields in the atmosphere and precipitation.

A relative high correlation between the SST anomalies and Southern Annular Mode (SAM) index was found in this same area in recent studies (LOVENDUSKI and GRUBER, 2005; SEN GUPTA and ENGLAND, 2005; TEIXEIRA *et al.*, 2005). These works have shown that the SAM influences many atmospheric variables including geopotential height, sea level pressure, air temperature, winds and cloud cover in the Southern Hemisphere. It leads to a modification in the Ekman transport and in the air–sea heat flux and, as a consequence, anomalies in the SST (LOVENDUSKI and GRUBER, 2005; SEN GUPTA and ENGLAND, 2005; TEIXEIRA *et al.*, 2005). Since SAM shows significant variability spanning from monthly to inter-annual time scales (THOMPSON and WALLACE 2000a, 2000b), the results suggest that the semi-annual signal in this area can be associated with SAM.

Significant values in the semi-annual amplitudes also appear near the BMC (site 8) due to mesoscale activity with temporal scales of less than a year (GARZOLI et a., 1987; LENTINI *et al.*, 2002; GONZALEZ-SILVERA, 2006). Analogous SST signals with this same period have been found in the East Australian Current near its separation latitude (RIDGWAY and GODFREY, 1997).

In the ocean portion between 24 and 40 ºS, there are small, but relevant values in the amplitude of the semi-annual cycle. This region is outside the influence of ocean currents and mesoscale processes, meaning that this variability can be related with the South Atlantic Convergence Zone (SACZ).

The SACZ is a climatological feature of this region during the austral summer and has been defined as an elongated convective band of clouds typically originating in the Amazon basin and extending across the southeast Brazil and offshore until it reaches the southeastern subtropical Atlantic Ocean (CARVALHO *et al.* 2004). The presence of the SACZ tends to create negative anomalies in the SST, possibly due to the reduction of the incident short-wave heat flux radiation and with increased latent heat flux, which are created by the increase of cloudiness and the larger SST contrast between the ocean and the atmosphere, respectively (CHAVES and NOBRE, 2004).

These cold anomalies present in the southern austral summer months coupled with the relative low temperatures during winter can lead to a variability with a six-month period, which therefore contributes to a semi-annual cycle in this region. The influence of the SACZ appears to slightly increase the SST annual amplitude (Fig. 6) in this same region.

The possible relationship between the SACZ and SAM with the SST semi-annual variability in the south Atlantic is an interesting topic which should be investigated further.

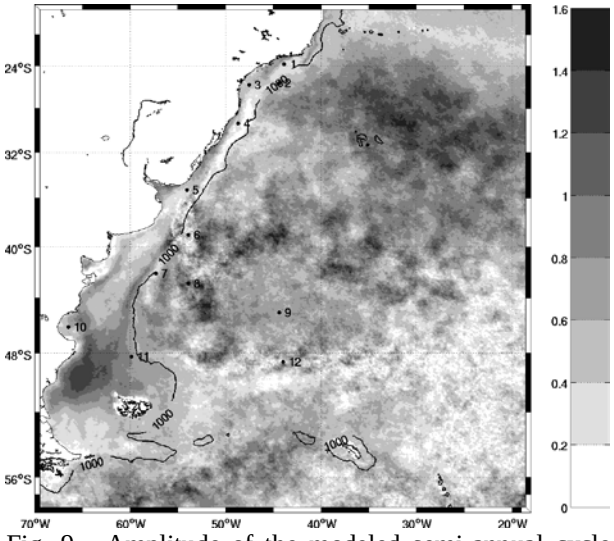

Fig. 9 - Amplitude of the modeled semi-annual cycle (units in ºC)

3.3 - Characterization of inter-annual variability*:*

We reconstructed the SST time series after subtracting the annual and semi-annual signals. The residual series contains only the mesoscale and inter-annual variability. These time series are subjected to a low pass filter (365 days) to separate the intra and the inter-annual variability. The residuals and filtered signals are shown in figure 12.

The variability associated with inter-annual phenomena is characterized by the standard deviation of the low pass filtered time series. The results are presented in figure 10. The region with the highest inter-annual variability is associated with the BMC (site 6), which has inter-annual variations of the same amplitude of its seasonal migration (OLSON *et al.*, 1988, LENTINI, 2002). There is yet to be a consensus regarding the causes of this variability which may be related to local or remote variations in wind pattern, variability in the BC and/or MC transport, ACC dynamics, or still to BC and MC meanders (OLSON *et al.*, 1988; MATANO *et al*, 1993; GARZOLI and GIULIVI, 1994; GONI *et al.*, 1996; LENTINI, 2002; LENTINI *et al.*, 2002, 2006).

The ACC (site 12) has significant inter-annual variability values (Fig. 10). Since the MC is formed as a branch of the ACC (PETERSON and STRAMMA, 1991), variations in the latter may lead to variations in the MC and consequently, in the BMC (LENTINI, 2002). Here we suggest that, this phenomenon may be associated with SAM, which also contains an inter-annual variability and has been shown to influence the ACC (HALL and VISBECK, 2002).

The Argentine shelf and the Santos Bay (sites 1 to 5 and coastal area between 24 - 28º S) also show relative high values in the inter-annual band which may be related to non-seasonal variations in La Plata river discharge. LENTINI *et al.* (2001) using thirteen years of weekly composite AVHRR images observed a total of

thirteen cold anomalies and seven warm anomalies over the southeastern South American continental shelf during and immediately after ENSO-related events. Such events influenced the SST anomalies over the shelf throughout the year and impacted local fisheries, despite their relative short duration (LENTINI *et al.*, 2001). Our analysis may capture the inter-annual variability of these ENSO-related events; despite the database herein used has duration of 9 years.

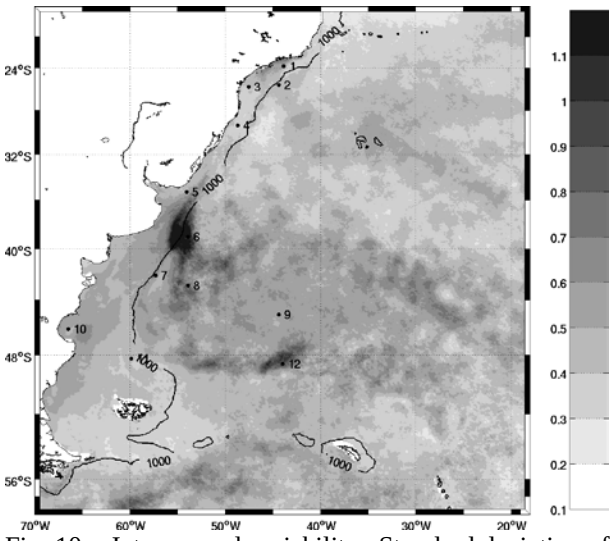

Fig. 10 - Inter-annual variability. Standard deviation of the SST residuals low-pass filtered (See text for details). Units in ºC

3.4 - The intra-annual signal

After the foregoing analysis, the inter-annual contribution is removed from the SST residuals. The signal left behind basically contains the mesoscale activity and the intra-annual variability (excluding the semi-annual period) plus the sampling noise. The sampling noise is assumed to have a normal random distribution on a pixel basis and thus is expected to cancel out during the analysis. Figure 11 shows the variance of the intra-annual signal. The highest variance appears in regions where mesoscale activity is known to occur, such as the BMC (sites 6 and 8), ACC (site 12) and SAC (GARZOLI and BIANCHI, 1987; GARZOLI and GIULIVI, 1994; VIVIER and PROVOST, 1999; GARCIA *et al.* 2004; LENTINI *et al.*, 2001; 2002; 2006).

In the Argentine basin (site 9, ~ 45ºS - 44ºW), there is a variance minimum possibly associated to the semi-stationary large-scale feature known as the Zapiola Drift (DE MIRANDA *et al.*, 1999, SARACENO *et al.*, 2005). This feature was detected during the A11 hydrographic section of the WOCE program (SAUNDERS and KING, 1995) and in modeling studies carried out by De Miranda *et al.* (1999). It is associated to a topographic high of 1100 m occurring in an abyssal plain of 6000 m.

A minimum variance also is found in the same area using sea surface height anomaly data provided by altimeter sensors (FU *et al.*, 2001; SARACENO *et al.*, 2005).

The maximum in variance observed around the Zapiola Drift (site 12) is associated with the mesoscale dynamics of the BMC and to the Subantarctic Front between 48 and 50 ºS. In this area there is a bathymetric contour centered on 49 ºS and extending from 55 to 40 ºW, and down to the approximately 1000m depth, that can serve as a preferable pathway to the mesoscale events due to the conservation of potential vorticity (DE MIRANDA at al., 1999). Modeling studies (DE MIRANDA at al., 1999) suggested that these mesoscale events can maintain the anticyclone flow around the Zapiola Drift.

This flow has a mean barotropic transport higher than 100 Sv (SAUNDERS and KING, 1995) and may cause the dynamical isolation of the central region of the Zapiola Drift (FU *et al.*, 2001) which explains the minimum variance in the intra-annual signal.

Between 18º and 24 ºS in the South Brazil Bight (site 1), there is a local maximum in variance near 21 ºS, which may be caused by the shelf break upwelling induced by BC frontal meanders and vortices, combined to the bathymetric orientation (CAMPOS *et al.*, 1995, DE SOUZA and ROBSON, 2004).

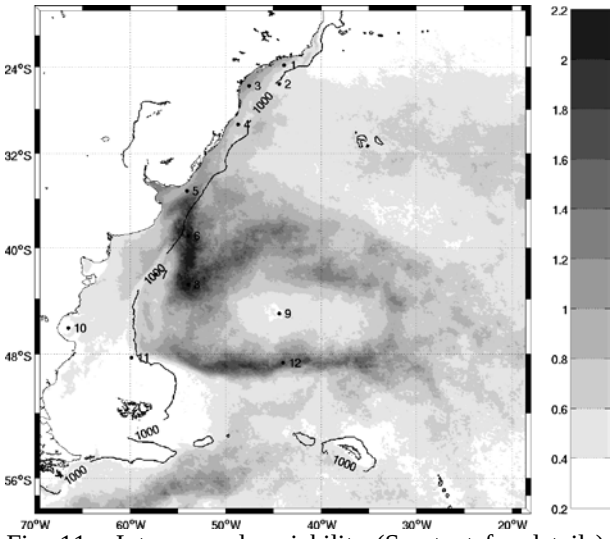

Fig. 11 - Intra-annual variability (See text for details). Units in ºC

The San Jorge Gulf (site 10) and the Valdez Peninsula present a local minimum in the intra annual variance. This is the result of the tidal mixing in the water column that tends to decrease the SST variability in all time scales.

Low values of variance are also found in the MC base (site 11 and region between 48º e 55º S and 50º and 70ºW), as a result of the steady mean flow of the MC in the area associated with homogeneous water characteristics which thus leads to a low SST variability.

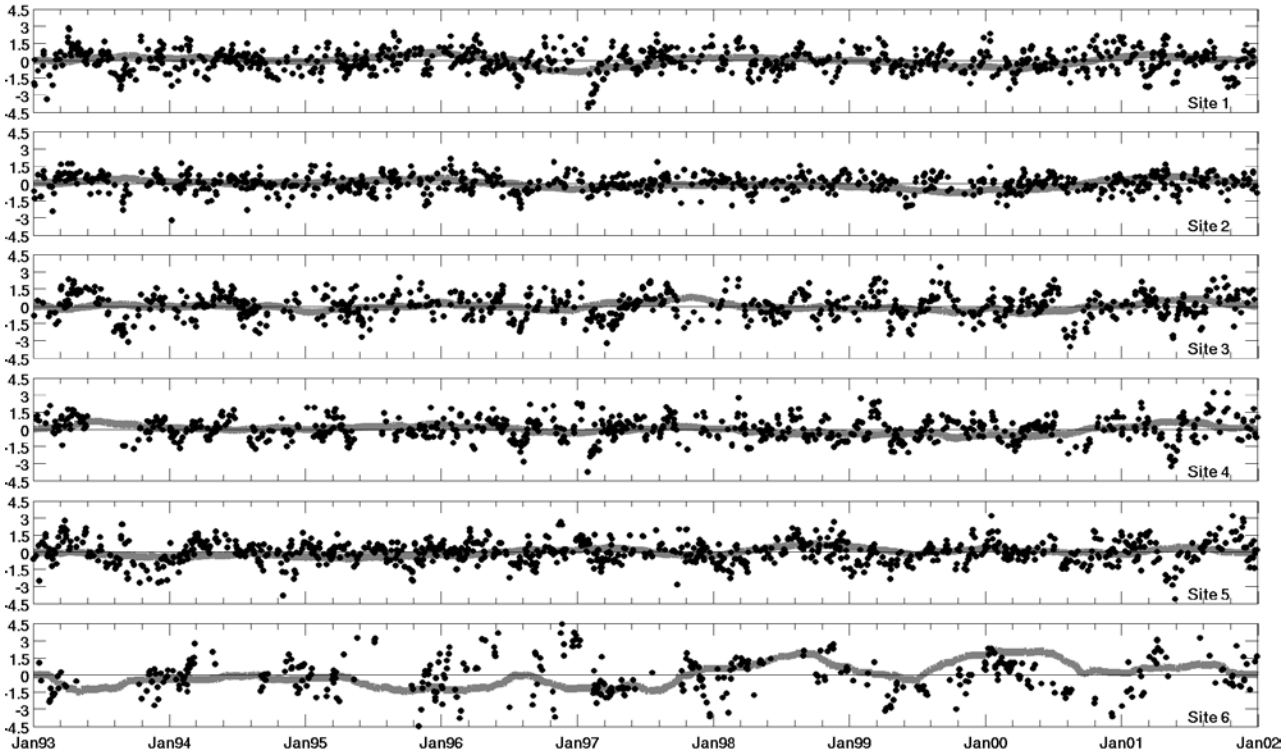

Fig. 12a - Original (circles) and filtered (solid lines) SST residuals for sites 1-12. The low-pass filter uses the objective mapping technique. See text for details. Units in ºC.

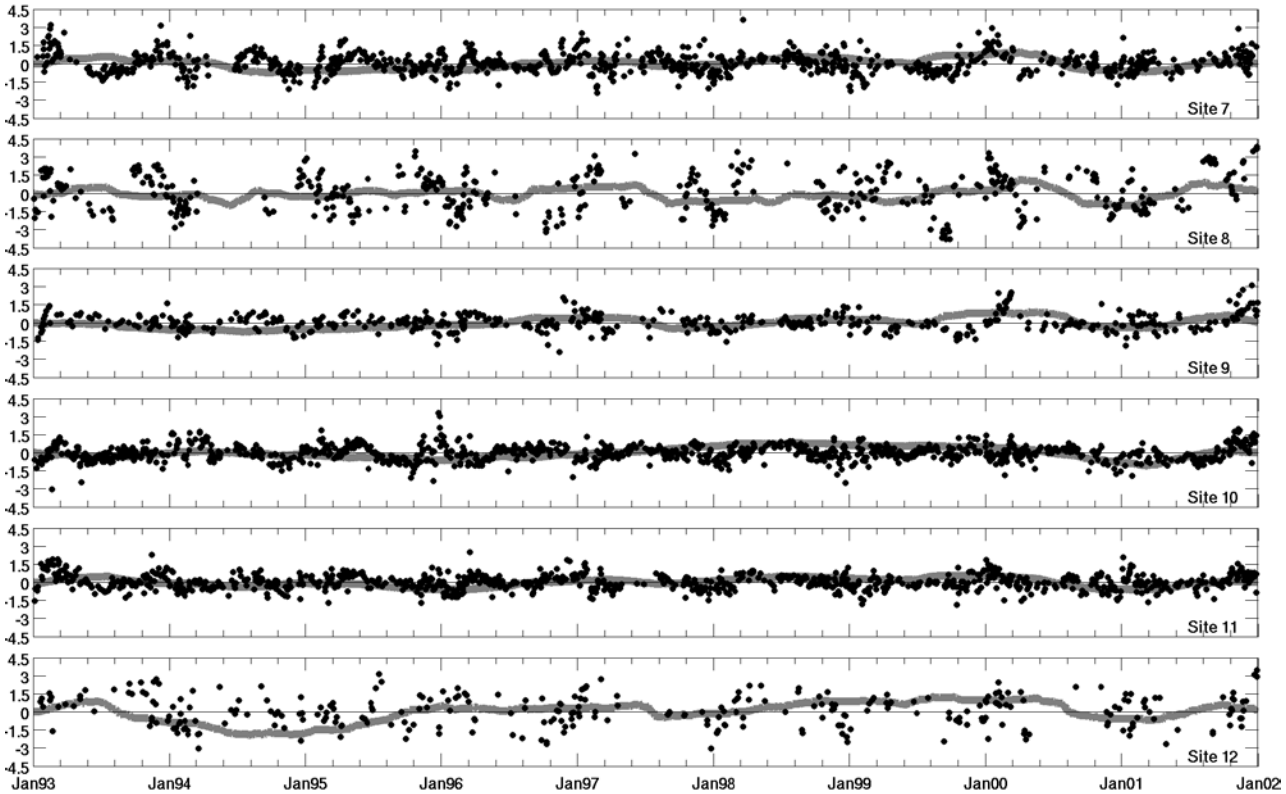

Fig. 12b - Original (circles) and filtered (solid lines) SST residuals for sites 1-12. The low-pass filter uses the objective mapping technique. See text for details. Units in ºC.

4. SUMMARY AND CONCLUSIONS

The deterministic part of the SST variability in the southwestern Atlantic Ocean is estimated by a simple harmonic model which calculates the annual and semi-annual components using a least-squares method. The seasonal cycle is removed from the original SST time series to investigate the inter-annual and mesoscale contributions to SST residual variability which is achieved by applying a low-pass filter (objective analysis with a cut-off = 365 days) on the 9 years of AVHRR/NOAA Pathfinder best SST images.

The relatively low numbers of valid data and the seasonal differences do not affect the deterministic part description and only marginally influence the inter-annual and intra-annual results presented.

The methods used to determinate annual and semi-annual amplitudes and phases in the present work follows the approach used in PODESTA et al. (1991), PROVOST et al. (1992) and LENTINI et al. (2001), but extend the results for a large domain and a significantly longer time series. Moreover, the higher resolution of SST data used allows the examination of small scale patterns along the coast. Furthermore, for the first time the SST variability of the off-shelf region between 18ºS and 34ºS was examined.

We found that the SST fields contain a strong annual cycle, explaining more than 85% of the signal variance in most parts of the study region. The amplitude of the annual cycle varies between 1° and 13°C with the highest values being found on the continental shelf and around the La Plata River mouth most probably as a consequence of the river runoff.

The mixing induced by the tidal currents in the San Jorge Gulf and the Valdez Peninsula decrease the SST variability throughout the year resulting in relative low values of the annual amplitude in these regions.

The phase of the annual cycle presents values between 25 and 70 days with respect to the 1st of January, occurring earlier over the continental shelf than offshore. This difference occurs due to the faster response of the shallow waters to variations in solar irradiance. New results show that the La Plata river discharge and the Melting waters from the Magellan Strait also influence the phase. The phase agreement between the BMC region and the continental shelf, evidence the advection of coastal waters to the oceanic region

The semi-annual component has a secondary importance, contributing to a maximum improvement of 3% in the determination coefficient between observed and modeled SST fields. The highest values (approximately 1.6º C) occur in the BMC region due the mesoscale activity that may have this same period of variability. High values of the semi-annual amplitude occur in the southwestern region of the study area. We suggest that these values may be associated with the SAM since previous works found a high correlation between SAM index and the SST anomalies in this region.

The oceanic portion between 24 and 32 ºS also, presents high values of semi-annual amplitude not yet described in the literature. We believe that theses high values are correlated to the SACZ variability, since it tends to create negative anomalies in the SST during the summer. These anomalies coupled to the low temperatures during the winter can lead to variability with a six-month period.

Although the method does not allow any inferences regarding the time scale contributing to the inter-annual and intra-annual variability, it provided important results about their spatial distribution.

The inter-annual variability is relatively minor over the domain (less than 1.2 ºC). The SST fields close to the ACC present high inter-annual variability, which may be related to the inter-annual band of variability of the SAM. The BMC region shows the highest inter-annual variability associated with changes in the position of the BMC zone. Since the SAM leads to changes in the wind stress field in the Southwestern Atlantic and the transport of the ACC it may change the MC and the BC. Based on these assumptions we speculate that the SAM may also be responsible for high values found in the BMC.

Significant values of inter-annual variability are also found in the Argentine shelf and the South Brazil Bight forced by variations in La Plata river discharge in the ENSO related years.

High intra-annual variability due to mesoscale activities occurs in the BMC, ACC and the SAC regions with values higher than 1.6 ºC. Through the methodology used here we were able to show the anti-cyclonic gyre around the Zapiola Drift using satellite-derived SST. The gyre appears as a minimal variance occurring around 45^0 S – 44^0 W. This flow is forced by the mesoscale events of the BMC and the ACC which appear as high variance values around the Zapiola Drift. The gyre tends to isolate the SST in the center of the drift resulting in the minimum intra-annual variance observed.

With the coefficients (phase and amplitude) of the annual and semi-annual harmonics, plus its mean value, it is possible to reconstruct the seasonal cycle of SST with a certain degree of precision. However, one must take into account that this statement should be applied with caution to regions where the non-deterministic signal plays an important role such as the mesoscale dynamics observed in the BMC, ACC Current and SAC.

The “Pathfinder best SST” dataset, version 4.1 developed by JPL, provides a high spatial and temporal resolution, which when combined to the pixel-to-pixel methodology presented here, allows to present some oceanographic features associated with SST not previously examined. Those features include phenomena ranging from coastal to large-scale with significant intra to inter-annual variability.

ACKNOWLEDGEMENTS

Resources for this study have been provided by the GOAL Project, part of the Brazilian Antarctic Survey (CNPq/PROANTAR/MMA, grant: 55.0370/02-1) and by the Federal University of Rio Grande (FURG). C. Teixeira was supported CNPq fellowship (grant: 180291/2003-3). We also thank John F. Middleton and John Luick for their comments and suggestions that added value to the manuscript.

REFERENCES

ACEITUANO, P. On the functioning of the southern oscillation in the south-american sector: 1. Surface climate. **Monthly Weather Review**, v. 116, n. 3, pp. 505-524, 1988.

CAMPOS, E. J. D.; GONCALVES, J. E.; IKEDA, Y. Water Mass Characteristics and Geostrophic Circulation in the South Brazil Bight - Summer of 1991 (Vol 100, Pg 18537, 1995). **Journal of Geophysical Research-Oceans**, v. 100, n. C11, pp. 22765-22765, 1995.

CARVALHO, L. M. V.; JONES, C.; LIEBMANN, B. The South Atlantic convergence zone: Intensity, form, persistence, and relationships with intraseasonal to inter-annual activity and extreme rainfall. **Journal of Climate**, v. 17, n. 1, pp. 88-108, 2004.

CHAVES, R. R.; NOBRE, P. Interactions between sea surface temperature over the South Atlantic Ocean and the South Atlantic Convergence Zone. **Geophysical Research Letters**, v. 31, n. 3, pp. L03204, 2004.

CHELTON, D. B.; SCHLAX, M. G. Estimation of time averages from irregularly spaced observations - with application to coastal zone color scanner estimates of chlorophyll concentration. **Journal of Geophysical Research-Oceans**, v. 96, n. C8, pp. 14669-14692, 1991.

CHELTON, D. B.; SCHLAX, M. G.; WITTER, D. L., et al. Geosat altimeter observations of the surface circulation of the Southern Ocean. **Journal of Geophysical Research**, v. 95, n. C10, pp. 17877-17903, 1990.

CRACKNELL, A. P.; HAYES, L. W. B. **Introduction To Remote Sensing**. London, UK, Taylor & Francis, 1991. 293.

DE MIRANDA, A. P.; BARNIER, B.; DEWAR, W. K. On the dynamics of the Zapiola Anticyclone. **Journal of Geophysical Research-Oceans**, v. 104, n. C9, pp. 21137-21149, 1999.

DE SOUZA, R. B.; ROBINSON, I. S. Lagrangian and satellite observations of the Brazilian Coastal Current. **Continental Shelf Research**, v. 24, n. 2, pp. 241-262, 2004.

DE SOUZA, R. B.; MATA, M. M.; GARCIA, C. A. E.; KAMPEL, M.; OLIVEIRA, E. N.; LORENZZETTI, J. A. Multi-sensor satellite and in situ measurements of a warm core ocean eddy south of the Brazil-Malvinas Confluence region. **Remote Sensing of Environment** v. 100, n 1, pp. 52-66. 2006

DIAZ, A. F.; STUDZINSKI, C. D.; MECHOSO, C. R. Relationships between precipitation anomalies in Uruguay and southern Brazil and sea surface temperature in the Pacific and Atlantic oceans. **Journal of Climate**, v. 11, n. 2, pp. 251-271, 1998.

EMERY, W. J.; THONSOM, R. E. **Data Analysis Methods in Physical Oceanography**. New York, Elsevier Science, 1998. 640 pp.

FU, L. L.; CHENG, B.; QIU, B. 25-Day Period Large-Scale Oscillations in the Argentine Basin Revealed by the TOPEX/Poseidon Altimeter. **Journal of Physical Oceanography.** v. 31, pp. 506-517, 2001

GARCIA, C. A. E.; SARMA, Y. V. B.; MATA, M. M., et al. Chlorophyll variability and eddies in the Brazil-Malvinas Confluence region. **Deep-Sea Research Part Ii-Topical Studies in Oceanography**, v. 51, n. 1-3, pp. 159-172, 2004.

GARZOLI, S. L.; BIANCHI, A. Time-Space Variability of the Local Dynamics of the Malvinas- Brazil Confluence as Revealed by Inverted Echo Sounders. **Journal of Geophysical Research-Oceans**, v. 92, n. C2, pp. 1914-1922, 1987.

GARZOLI, S. L.; GIULIVI, C. What Forces the Variability of the Southwestern Atlantic Boundary Currents. **Deep-Sea Research Part I-Oceanographic Research Papers**, v. 41, n. 10, pp. 1527-1550, 1994.

GLORIOSO, P. D. Temperature distribution related to shelf sea fronts on the Patagonian shelf. **Continental Shelf Research**, v. 7, n. 1, pp. 27-34, 1987.

GLORIOSO, P. D.; FLATHER, R. A. The Patagonian Shelf tides. **Progress in Oceanography**, v. 40, n. 1-4, pp. 263-283, 1997.

GONZALEZ-SILVERA, A.; SANTAMARIA-DEL-ANGEL, E.; MILLAN-NUNEZ, R. Spatial and temporal variability of the Brazil-Malvinas Confluence and the La Plata Plume as seen by SeaWiFS and AVHRR imagery. **Journal of Geophysical Research-Oceans**, v. 111, n. C6, pp., 2006.

GORDON, A. L. Brazil Malvinas Confluence - 1984. **Deep-Sea Research Part a-Oceanographic Research Papers**, v. 36, n. 3, pp. 359-384, 1989.

HALL, A.; VISBECK, M. Synchronous variability in the southern hemisphere atmosphere, sea ice, and ocean

resulting from the annular mode. **Journal of Climate**, v. 15, n. 21, pp. 3043-3057, 2002.

KILPATRICK, K. A.; PODESTA, G. P.; EVANS, R. Overview of the NOAA/NASA advanced very high resolution radiometer Pathfinder algorithm for sea surface temperature and associated matchup database. **Journal of Geophysical Research-Oceans**, v. 106, n. C5, pp. 9179-9197, 2001.

LEFEBVRE, W.; GOOSSE, H.; TIMMERMANN, R., et al. Influence of the Southern Annular Mode on the sea ice-ocean system. **Journal of Geophysical Research-Oceans**, v. 109, n. C9, pp., 2004.

LEGECKIS, R.; GORDON, A. L. Satellite-Observations of the Brazil and Falkland Currents - 1975 to 1976 and 1978. **Deep-Sea Research Part a-Oceanographic Research Papers**, v. 29, n. 3, pp. 375-401, 1982.

LENTINI, C. A. D. The annual cycle of satellite derived sea surface temperature on the western South Atlantic shelf. **Brazilian Journal of Oceanography**, v. 48, n. 2, pp. 93-105, 2000.

LENTINI, C. A. D. The role of the Brazil-Malvinas confluence on regional mesoscale dynamics and climate. Coral Gables, Florida, Univ. de Miami. Phd**:** 192, 2002.

LENTINI, C. A. D.; GONI, G. J.; OLSON, D. B. Investigation of Brazil Current rings in the confluence region. **Journal of Geophysical Research-Oceans**, v. 111, n. C6, pp., 2006.

LENTINI, C. A. D.; OLSON, D. B.; PODESTA, G. P. Statistics of Brazil Current rings observed from AVHRR: 1993 to 1998. **Geophysical Research Letters**, v. 29, n. 16, pp., 2002.

LENTINI, C. A. D.; PODESTA, G. G.; CAMPOS, E. J. D., et al. Sea surface temperature anomalies on the Western South Atlantic from 1982 to 1994. **Continental Shelf Research**, v. 21, n. 1, pp. 89-112, 2001.

LOVENDUSKI, N. S.; GRUBER, N. Impact of the Southern Annular Mode on Southern Ocean circulation and biology. **Geophysical Research Letters**, v. 32, n. 11, pp., 2005.

MATANO, R. P. On the Separation of the Brazil Current from the Coast. **Journal of Physical Oceanography**, v. 23, n. 1, pp. 79-90, 1993.

MEREDITH, M. P.; WOODWORTH, P. L.; HUGHES, C. W., et al. Changes in the ocean transport through Drake Passage during the 1980s and 1990s, forced by changes in the Southern Annular Mode. **Geophysical Research Letters**, v. 31, n. 21, pp., 2004.

OLSON, D. B.; PODESTA, G. P.; EVANS, R. H., et al. Temporal Variations in the Separation of Brazil and Malvinas Currents. **Deep-Sea Research Part a-Oceanographic Research Papers**, v. 35, n. 12, pp. 1971-1990, 1988.

PETERSON, R. G.; STRAMMA, L. Upper-Level Circulation in the South-Atlantic Ocean. **Progress in Oceanography**, v. 26, n. 1, pp. 1-73, 1991.

PIOLA, A. R.; CAMPOS, E. J. D.; MOLLER, O. O., et al. Subtropical Shelf Front off eastern South America. **Journal of Geophysical Research-Oceans**, v. 105, n. C3, pp. 6565-6578, 2000.

PIOLA, A. R.; MATANO, R. P.; PALMA, E. D., et al. The influence of the Plata River discharge on the western South Atlantic shelf. **Geophysical Research Letters**, v. 32, n. 1, pp., 2005.

PODESTA, G. P.; BROWN, O. B.; EVANS, R. H. The Annual Cycle of Satellite-Derived Sea-Surface Temperature in the Southwestern Atlantic-Ocean. **Journal of Climate**, v. 4, n. 4, pp. 457-467, 1991.

PROVOST, C.; GARCIA, O.; GARCON, V. Analysis of Satellite Sea-Surface Temperature Time-Series in the Brazil-Malvinas Current Confluence Region - Dominance of the Annual and Semiannual Periods. **Journal of Geophysical Research-Oceans**, v. 97, n. C11, pp. 17841-17858, 1992.

RIDGWAY, K. R.; DUNN, J. R.; WILKIN, J. L. Ocean interpolation by four-dimensional weighted least squares - application to the waters around Australasia. **Journal of Atmospheric and Oceanic Technology**, v. 19, n. 9, pp. 1357-1375, 2002.

ROMERO, S. I.; PIOLA, A. R.; CHARO, M., et al. Chlorophyll-alpha variability off Patagonia based on SeaWiFS data. **Journal of Geophysical Research-Oceans**, v. 111, n. C5, pp., 2006.

SAUNDERS, P. M.; KING, B. A. Bottom currents derived from a ship-borne ADCP on WOCE cruise A11 in the South-Atlantic. **Journal of Physical Oceanography**, v. 25, n. 3, pp. 329-347, 1995.

SECKEL, G. R.; BEAUDRY, F. H. Radiation from sun and sky over North Pacific ocean. **Transactions-American Geophysical Union**, v. 54, n. 11, pp. 1114-1114, 1973.

SEN GUPTA, A.; ENGLAND, M. H. Coupled ocean-atmosphere-ice response to variations in the Southern Annular Mode. **Journal of Climate**, v. 19, n. 18, pp. 4457-4486, 2006.

SMITH, E. Satellite-derived sea surface temperature data available on-line. **Eos, Transactions American Geophysical Union**, v. 77, n. 14, pp. 135-135, 1996.

SOARES, I.; MOLLER, O. Low-frequency currents and water mass spatial distribution on the southern Brazilian shelf. **Continental Shelf Research**, v. 21, n. 16-17, pp. 1785-1814, 2001.

TEIXEIRA, C. E. P.; LENTINI, C. A. D.; MATA, M. M. The influence of the Southern Annular Mode (SAM) over the sea surface temperatures in the southwestern Atlantic. **Proc. 8th International Conference on Southern Hemisphere Meteorology and Oceanography (ICSHMO)**, Foz do Iguaçu, INPE,2006.

THOMPSON, D. W. J.; WALLACE, J. M. Annular modes in the extratropical circulation. Part I: Month-to-month variability. **Journal of Climate**, v. 13, n. 5, pp. 1000-1016, 2000.

THOMPSON, D. W. J.; WALLACE, J. M.; HEGERL, G. C. Annular modes in the extratropical circulation. Part II: Trends. **Journal of Climate**, v. 13, n. 5, pp. 1018-1036, 2000.

TOMCZAK, M.; GODFREY, J. S. **Regional Oceanography: An Introduction**. Oxford, Pergamon, 1994. 442.

VAN LOON, H. The Half-Yearly Oscillations in Middle and High Southern Latitudes and the Coreless Winter, **Journal of the Atmospheric Sciences**. 24: 472-486, 1967

VENEGAS, S. A.; MYSAK, L. A.; STRAUB, D. N. Atmosphere-ocean coupled variability in the South Atlantic. **Journal of Climate**, v. 10, n. 11, pp. 2904-2920, 1997.

Vivier, F.; Provost C.. Direct velocity measurements in the Malvinas Current. **Journal of Geophysical Research-Oceans,** v.104, n. C9,pp. 21083-21103, 1999.

WALKER, A. E.; WILKIN, J. L. Optimal averaging of NOAA/NASA pathfinder satellite sea surface temperature data. **Journal of Geophysical Research-Oceans**, v. 103, n. C6, pp. 12869-12883, 1998.